Physica E 126 (2021) 114417

Contents lists available at ScienceDirect

Physica E: Low-dimensional Systems and Nanostructures

journal homepage: http://www.elsevier.com/locate/physe

Sustainable synthesis of carbon quantum dots from banana peel waste using hydrothermal process for *in vivo* bioimaging☆

Raji Atchudan [a,*,1], Thomas Nesakumar Jebakumar Immanuel Edison [a,1], Mani Shanmugam [d,1], Suguna Perumal [b,1], Thirunavukkarasu Somanathan [c,1], Yong Rok Lee [a,**]

[a] School of Chemical Engineering, Yeungnam University, Gyeongsan, 38541, Republic of Korea
[b] Department of Applied Chemistry, Kyungpook National University, Daegu, 41566, Republic of Korea
[c] Department of Chemistry, School of Basic Sciences, Vels Institute of Science, Technology & Advanced Studies (VISTAS), Chennai, 600117, India
[d] Department of Science and Humanities, Institute of Aeronautical Engineering, Dundigal, Hyderabad, 500043, India

ARTICLE INFO

Keywords:
Banana peel waste
Carbon quantum dots
Hydrothermal method
Nematodes
Bioimaging

ABSTRACT

Banana peel is a common solid biowaste. This paper reports a sustainable synthesis of carbon quantum dots (CQDs) from banana peel waste by a simple hydrothermal method. The resulting CQDs have a narrow size distribution, and the average particle size was measured as 5 nm. The nitrogen-containing and oxygen-containing functionalities on/in the surface of carbon structure were observed in the resulting CQDs. CQDs emit intense blue fluorescence under the excitation of UV-light (365 nm) with a good quantum yield of 20% without any surface passivation chemicals. Besides, CQDs exhibit excellent water solubility and excitation-dependent emission performance. Furthermore, the banana peel waste-derived CQDs had almost no photobleaching under UV-light irradiation for a long-time, suggesting that they have high photostability. Since no chemical reagent was involved in the synthesis of CQDs, the synthesized CQDs were confirmed to have lower toxicity for nematodes even at a high concentration of 200 μg mL^{-1}. Because of the intense fluorescence with excellent fluorescence stability and biocompatibility, CQDs can be used for bioimaging in nematodes. The CQDs efficiently stained into the whole body of the nematodes and brightly illuminated the multicolor by varying the excitation wavelength. Therefore, fluorescent CQDs would be a great potential candidate for bioimaging applications.

1. Introduction

Carbon quantum dots (CQDs) are a new class of zero-dimensional carbon nanoparticles that are mainly comprised of carbon with a size below 10 nm. They have earned great attention because of their wide range of applications such as medical diagnosis, photocatalysis, fluorescent sensing, optoelectronic devices, cellular labeling, and bioimaging due to their multicolor optical properties, excellent water solubility, high chemical stability, low toxicity, and outstanding biocompatibility. Since semiconductor quantum dots have notable cytotoxicity, biomass CQDs are considered to be a potential alternative for them towards biological applications [1–8]. Hence, great efforts have been focused on the favorable synthesis of CQDs and developing CQDs for the various applications. Numerous top-down (arc-discharge, laser ablation, and electrochemical oxidation) and bottom-up (microwave, ultrasonic, solvothermal, hydrothermal treatment, and so on) methods/strategies have been reported so far for the synthesis of CQDs [9–12]. However, most of the top-down approaches are burdened by manufacturing difficulties, largescale production expenses due to the use of costly equipment and tedious processes. In contrast, bottom-up approaches are simple and environmentally friendly. Among these reported bottom-up approaches, the hydrothermal method attracted much attention due to its eco-friendly, facile, cost-effective, and mass production [13]. In particular, hydrothermal methods using natural precursors to produce CQDs have been widely reported because of their green chemistry nature [14–17]. A lot of precursors were used as the

☆ Electronic Supplementary Information (ESI): Instrumentation methods, quantum yield measurement, photobleaching stability measurement, fluorescence study, nematode killing assay, fluorescent staining and imaging analysis of the synthesized CQDs.

* Corresponding author.
** Corresponding author.
E-mail addresses: atchudanr@yu.ac.kr (R. Atchudan), yrlee@yu.ac.kr (Y.R. Lee).

[1] Authors contributed equally to this work.

https://doi.org/10.1016/j.physe.2020.114417
Received 14 April 2020; Received in revised form 9 July 2020; Accepted 14 August 2020
Available online 6 September 2020

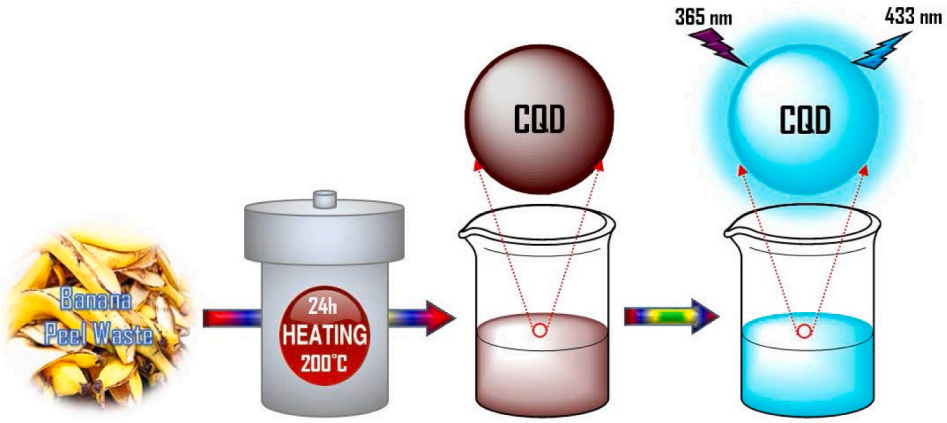

Scheme 1. Schematic illustration of the formation of fluorescent CQDs from banana peel waste via hydrothermal treatment.

starting materials for the synthesis of CQDs. In general, organic molecules are selected as the most reliable precursors to form high-quality CQDs with good quantum yield. However, the toxicity of the aromatic hydrocarbon precursors severely limited their widespread use. Therefore, developing non-toxic precursors for the production of CQDs instead of toxic organic precursors are still desirable. Some effort has been made to utilize a wide range of easily available natural biomass/biowaste such as vegetables, fruits, milk, and even waste as precursors due to their renewable, non-toxic, cost-effective, and biocompatible properties [18]. The further doping of heteroatoms into the carbonaceous framework and the surface passivation can substantially enhance the fluorescence activity of CQDs [19,20]. If the heteroelement doping and passivation can proceed simultaneously, highly fluorescent CQDs can be prepared more facilely. Besides, natural materials usually contain multifarious heteroatoms, so CQDs synthesized from these materials are always packed with various surface groups and possess unique properties without further passivation or modification [21]. Therefore, many efforts have been devoted to synthesize CQDs from various natural biomass/biowaste.

In this work, banana peel waste was adopted as precursors to prepare carbon quantum dots (CQDs) through facile and green hydrothermal methods without any passivates or additives. The synthesized CQDs exhibited excellent fluorescence properties, good water-solubility, acceptable quantum yield, low toxicity, good biocompatibility, and robust resistance against photobleaching were obtained. The CQDs were characterized by transmission electron microscopy (TEM), attenuated total reflectance-Fourier transforms infrared (ATR-FTIR) spectroscopy, X-ray photoelectron spectroscopy (XPS), UV–vis and fluorescence spectra. Under different excitation wavelengths (λ_{ex}), they exhibited multi-emission fluorescence. The toxicity of CQDs against nematodes was studied through a standard MTT assay. The CQDs served as efficient probes for cellular multicolor imaging.

2. Experimental

2.1. Materials

Dwarf banana fruits were purchased from the food market, Republic of Korea. S-basal buffer, sodium azide (NaN_3), and 3-(4,5-Dimethylthiazol-2-yl)-2,5-diphenyltetrazolium bromide (MTT) were purchased from Sigma-Aldrich, Republic of Korea. All the chemicals were used as received and the deionized (DI) water was used throughout this study.

2.2. Synthesis of carbon quantum dots

The fluorescent CQDs were synthesized from banana peel waste via a simple hydrothermal method. Briefly, the banana peel waste was ground well with DI water and transferred into a Teflon lined stainless steel autoclave. The autoclave was tightly sealed then placed in a domestic hot air oven, and heated for 24 h at 200 °C. Then obtained brownish-yellow crude product was filtered through a mixed cellulose ester membrane (0.22 μm) to remove the larger substances (particles). Finally, the clear brownish-yellow (CQDs) solution was collected and the supernatant liquid was showing fluorescent properties. The obtained CQDs solution was stored in a refrigerator and maintained at 4 °C until used. To meet the needs of characterization, sometimes it needed to be

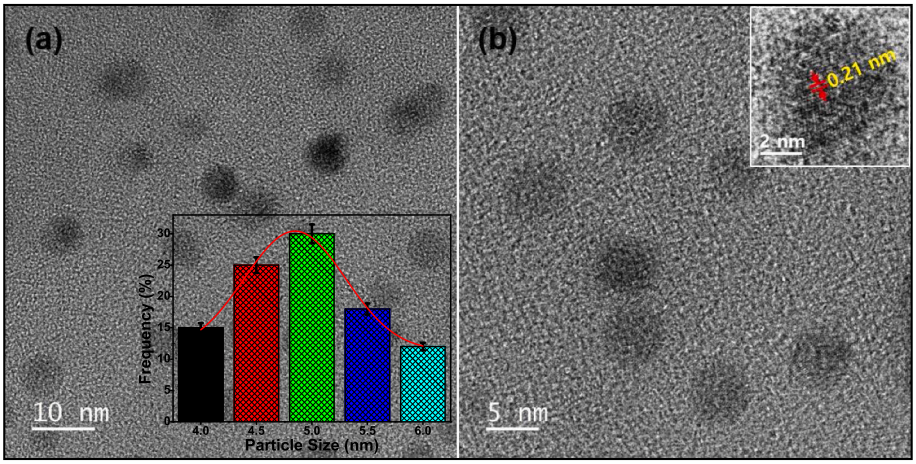

Fig. 1. (a) TEM image of synthesized CQDs and (b) HRTEM image of synthesized CQDs. Inset (a) is a particle size distribution graph of CQDs.

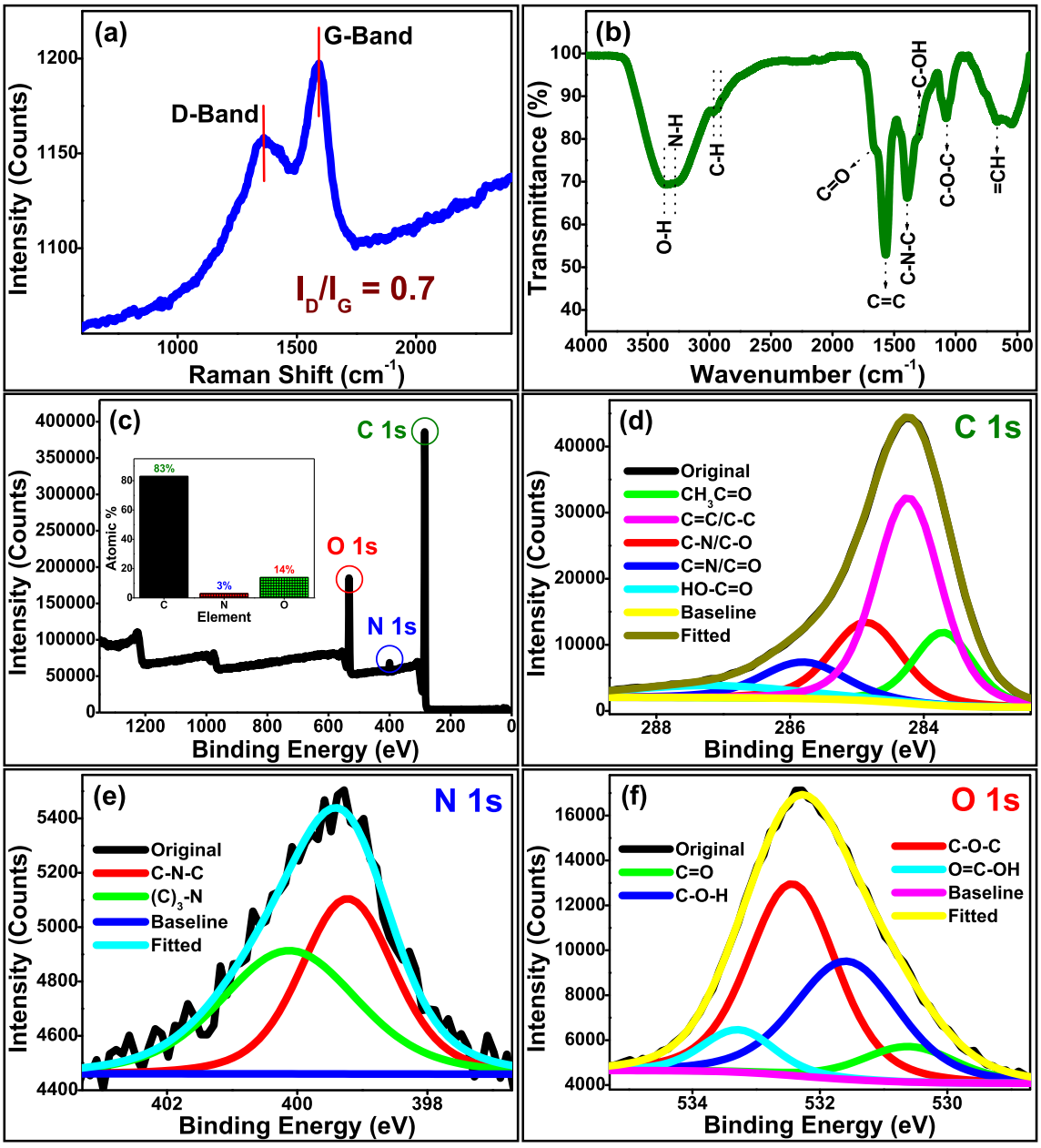

Fig. 2. (a) Raman spectrum and (b) ATR-FTIR spectrum of synthesized CQDs. (c) XPS survey spectrum, (d) high-resolution C 1 s spectrum, (e) high-resolution N 1 s spectrum and (f) high-resolution O 1 s spectrum of synthesized CQDs.

prepared as a solid, for that sample was prepared as follows: A part of CQDs solution was taken out and vacuum freeze-dried for 48 h to obtain the solid brown powder product. They were used for further characterization and applications.

3. Results and discussion

The fluorescent CQDs were synthesized from banana peel waste via a simple hydrothermal method and the illustration of the formation as shown in Scheme 1. The morphology and size of the synthesized CQDs were examined by TEM and HRTEM. Fig. 1(a) shows the particle size range within the limits of 4–6 nm and the average diameter of particles was about 5 nm suggesting the particle is in narrow distribution with a spherical shape. The particle size histogram of synthesized CQDs is shown as the inset of Fig. 1(a). As shown in the graph, the particle sizes are mainly distributed from 4 to 6 nm and the average diameter of CQDs is around 5 nm, determined by fitting a Gaussian model. The HRTEM images (Fig. 1(b)) reveals that the synthesized CQDs are having good lattice fringes, which imply a good crystalline structure. The inner part of CQDs is highly crystalline as compared to the outer surface of CQDs which confirms from the inset Fig. 1(b). CQDs showed lattice spacing approximately 0.21 nm is due to the (1 0 0) plane of typical graphene. The XRD pattern of the synthesized CQDs (Fig. S1) shows the peaks centered at $2\theta = 23$ and 42.5° corresponding to the (0 0 2) and (1 0 0) planes of carbon-based materials, respectively [22]. The CQDs have a predominantly graphitic structure with the interlayer spacing of 0.38 and 0.21 nm are attributed to the (0 0 2) and (1 0 0) planes, respectively. The d-spacing is larger than the distance between the (0 0 2) planes in typical bulk graphite (~0.34 nm) which is due to the presence of several functionalities and or miners turbostratic/amorphous carbon phase/structure. The calculated d-spacing of 0.21 nm as corresponds to the plane (1 0 0) facets of carbon-based materials, agrees well with HETEM results. Besides, broad peaks were observed in the XRD patterns, confirming the smaller particles and or amorphous materials. The functional

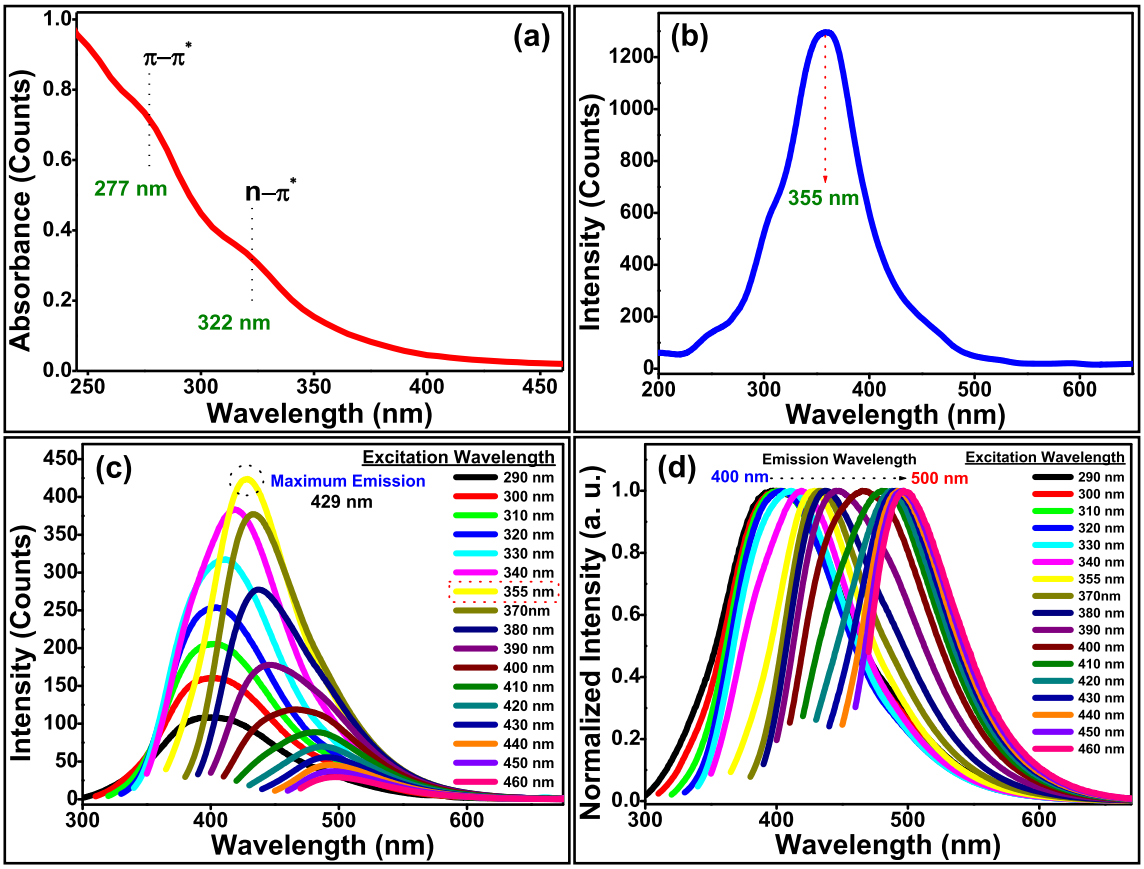

Fig. 3. (a) UV–Vis spectrum, (b) fluorescence excitation spectrum, (c) excitation-dependent fluorescence emission spectra and (d) excitation-dependent fluorescence emission normalized spectra of synthesized CQDs.

groups on the surface of the CQDs are resultant of the slight amorphous phase. Furthermore, the graphitization/crystallization of the synthesized CQDs were examined by the Raman spectroscopy technique and the corresponding Raman spectrum is presented in Fig. 2 (a). Raman spectrum of synthesized CQDs showed two broad peaks at 1360 and 1592 cm^{-1}. The peaks 1360 cm^{-1} is conventionally referred to as the D-band, which is known to become defective/disordered crystallites of graphite [23]. The high-frequency peak at 1592 cm^{-1} is conventionally referred to as the G-band of graphite, assigned to the C–C in-plane stretching vibration (E_2g) of graphite [24]. Hence, the D to G band ratio (I_D/I_G) represents the concentration of defects in the graphitic structure, and the low value of I_D/I_G in CQDs implies the integrity of the graphitic shells is sufficiently high to protect the core material well from corrosion and oxidation. The I_D/I_G ratio of the CQDs is ~0.7, which reveals that the CQDs are with acceptable graphitization [25]. Contribution from functional groups and or amorphous carbon during the synthesis cannot be excluded and thus leads to broad D-band.

It was believed that the surface of CQDs might have enormous functionalities. The functionalities of the CQDs were characterized by FTIR spectroscopy. In the ATR-FTIR spectrum (Fig. 2(b)), the peaks

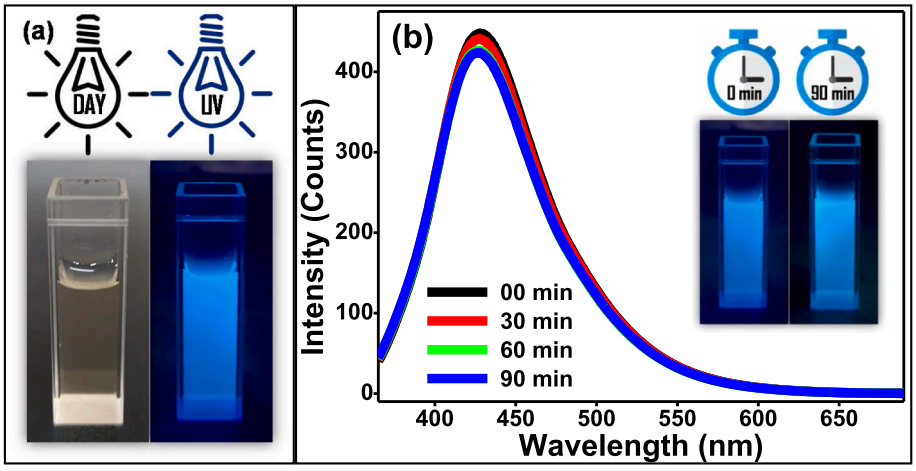

Fig. 4. (a) Optical images of synthesized CQDs under the daylight and UV light and (b) fluorescence spectra of synthesized CQDs aqueous solution at different irradiation times of 365 nm UV light (Inset: Optical images of CQDs solution at 0 and 90 min irradiations).

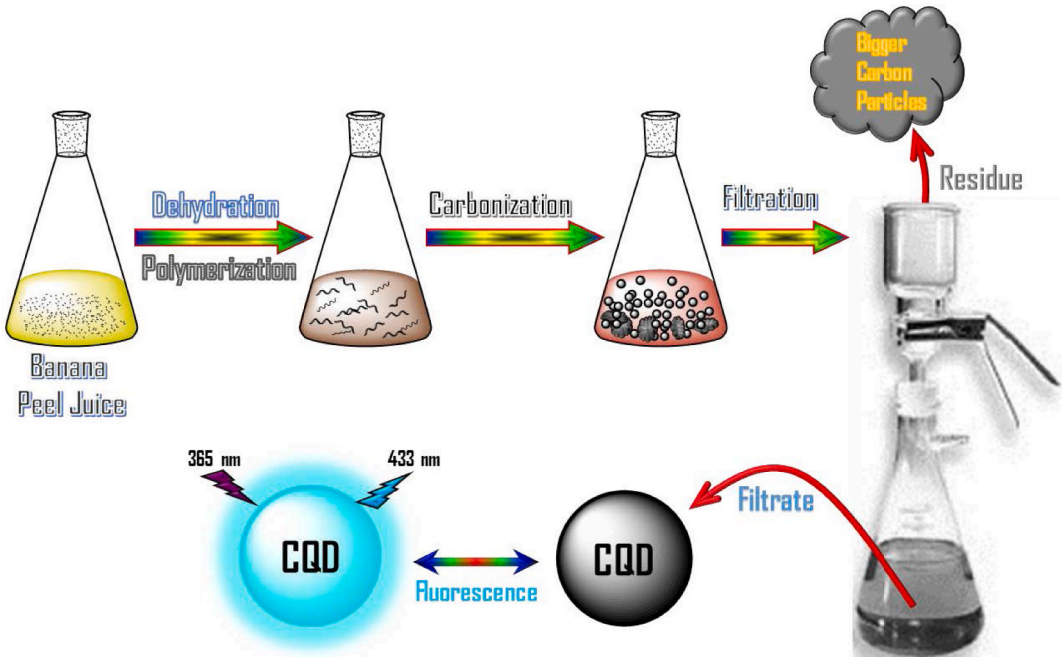

Scheme 2. Plausible formation mechanism of CQDs from the banana peel by hydrothermal process.

observed around 3366 and 3277 cm^{-1} are ascribed to the stretching vibrations of –OH and N–H groups, respectively [26]. C–H as-symmetric and symmetric stretching vibrations were observed at 2936 and 2868 cm^{-1}, respectively [2]. The peaks located around 1686, 1570, 1395, 1290 and 1072 cm^{-1} correspond to the respective functional groups C═O, C═C, C–N–C, C–OH and C–O–C reveals the presence of nitrogen and oxygen element in/on the surface of CQDs [27,28]. The peak observed at 670 cm^{-1} can be assigned to the methylene symmetric bending vibrations in the CQDs. All these functionalities contribute to the excellent aqueous solubility of CQDs and suggested that the prepared CQDs will be useful for further modifications and biological applications. Furthermore, XPS measurement was performed to determine the surface states including functionalities and elemental composition of CQDs. The full-scan XPS spectrum (Fig. 2(c)) shows three bands at around 285, 400 and 533 eV reveals the existence of carbon (C 1s), nitrogen (N 1s) and oxygen (O 1s) respectively, with an atomic ratio of C/N/O is 83/3/14 as calculated from the survey spectrum. The C 1s core-level XPS spectrum (Fig. 2(d)) can be deconvoluted into five contributions at 283.7, 284.2, 284.9, 285.8 and 287.3 eV, which are associated with carbon in the states of CH_3C═O, C–C/C═C, C–N/C–O, C═N/C═O and HO–C═O, respectively [29,30]. In the expanded XPS spectrum (Fig. 2(e)), N 1s core level can be deconvoluted into two peaks at 399.2 and 400.1 eV suggesting nitrogen exists mostly in the form of C–N–C and $(C)_3$–N bonds, respectively [31–33]. As shown in Fig. 2(f), the O 1s core-level XPS spectrum can be deconvoluted into four contributions at 530.6, 531.6, 532.4, and 533.3 eV which can be assigned to C═O, C–OH, C–O–C and HO–C═O, respectively [34,35]. It can be concluded that CQDs have a variety of polar groups including hydroxyl, alkyl, and carboxyl. The presence of these functionalities in the CQDs is responsible for their good dispersion/solubility in water.

Optical properties are the crucial factor to decide the optical-based applications. Hence, the hydrothermal duration has been varied for the synthesis of CQDs to explore an excellent fluorescence property. Fig. S2 displays the fluorescence spectra of CQDs prepared at different times (12, 24, and 48 h). The fluorescence intensity of CQDs was gradually enhanced with increasing the hydrothermal duration. However, the fluorescence intensity of CQDs at 24 h significantly improved compared to 12 h reaction time, also insignificant enhancement was observed for 48 h when compared to 24 h. Hence, we optimized 24 h is an optimum reaction time for the synthesis of highly fluorescent CQDs and utilized for the characterization and suitable applications. The optical properties of synthesized CQDs were confirmed by the UV–vis and fluorescence spectra. The UV–vis absorbance curve (Fig. 3(a)) of the synthesized CQDs shows the broad absorption ranges at 277 and 322 nm in the UV region which are correlated to the typical $\pi \rightarrow \pi^*$ transition band of the aromatic (C═C) sp^2 hybrid orbitals and $n \rightarrow \pi^*$ transition

Table 1
Comparison of optical properties of carbon dots with quantum yield from various precursors and various synthesis methods.

Carbon Precursor (Resulting Material)	Synthesized Method	λ_{ex} (nm)	λ_{em} (nm)	QY (%)	Application	Reference
Magnolia flower (MF-CQDs)	Hydrothermal	350	435	8.13	Detection of Fe^{3+} ions	[42]
Spinach (R-CDs)	Solvothermal	440	680	15.34	Bioimaging	[43]
Syringa Obtata Lindl (B-CDs)	Hydrothermal	450	520	12.4	Sensors and Cells imaging	[44]
Waste chimney oil (COC-dots)	Ultrasonication	380	472	7.5	Sensors, bio-labeling, and ink	[45]
Manilkara zapota fruit (C-dots)	Solvothermal	420	515	7.9	Bioimaging	[46]
Solanum Lycopersicum (B, G, Y-CDs)	Solvothermal	360	450	12.7	Sensors and Bioimaging	[47]
Protein (P-CDs)	Microwave	310	414	6.81	–	[48]
Nannochloropsis (N–S–C-Dots)	Microwave (HTL)	340	430	13.71	Bioimaging	[49]
Bamboo leaves (CD hybrids)	Hydrothermal	400	493	4.7	Detection of Pb^{2+} ions	[50]
Rice residue (N-CQDs)	Hydrothermal	440	500	23.48	Detection of Fe^{3+} ions	[51]
Unripe peach (N-CDs)	Hydrothermal	310	400	15	ORR	[35]
Malus floribunda (N-CDs)	Hydrothermal	335	406	19	Bioimaging	[23]
Banana Peel (CQDs)	Hydrothermal	355	429	20	Bioimaging	Present work

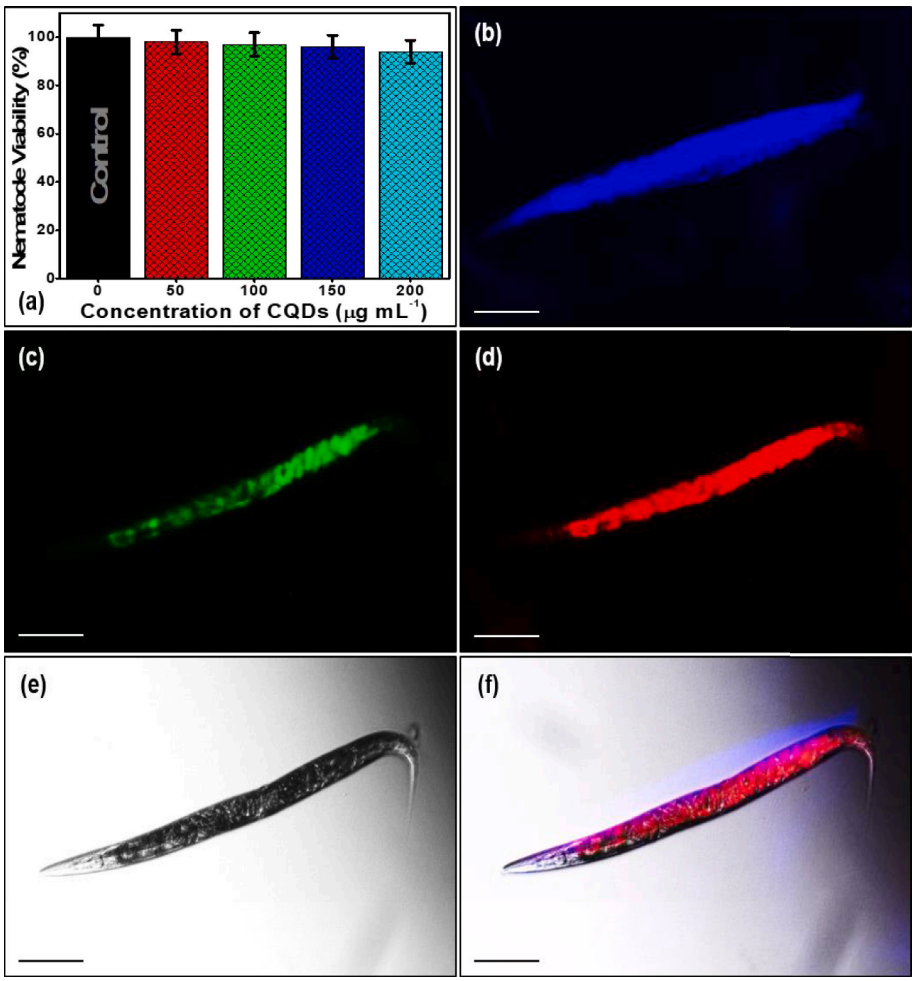

Fig. 5. (a) Toxicity assay of nematode incubation with different concentrations of synthesized CQDs. Multicolor imaging of *in vivo* model nematode incubation with CQDs (100 μg mL^1) under the excitation wavelength of (b) 400 nm, (c) 470 nm, (d) 550 nm, (e) bright-field (BF) and (f) merge (overlap). Live nematodes were immobilized using 0.05% sodium azide (NaN_3) for imaging under fluorescence filters.

band of the (C═O) sp^3 hybrid orbitals (functional group on the surface of CQDs), respectively [36]. Fig. 3(b) shows the fluorescence excitation spectrum of CQDs in aqueous solution reveals that the maximum excitation is centered around 355 nm. Fig. 3(c) displays the fluorescence emission spectra of CQDs aqueous solution at the different excitation wavelengths. The fluorescence intensities of CQDs are enhanced with increasing excitation wavelength up to 355 nm beyond that decreased gradually. When the excitation wavelength is 355 nm, CQDs showed the strongest fluorescence. Besides, it is interesting that the fluorescence emission spectra exhibit a redshift (longer emission wavelength, λ_{em}) with respect to the increment of the excitation wavelength ranging from 290 to 460 nm, which is vividly seen in the normalized fluorescence emission spectra (Fig. 3(d)). The synthesized CQDs should be noted that the fluorescence emission properties concerning the excitation wavelength. The origin of the optical properties of CQDs is still hotly debated and is not yet well understood. Therefore, mechanisms involving quantum confinement, surface traps, the formation of aromatic structures, and the recombination of excitons have been proposed [37,38]. A tunable and stable fluorescence emission is preferred for practical bioimaging. Hence, the synthesized CQDs are more suitable for cell imaging applications.

The fluorescence photostability of the CQDs is one of the crucial parameters for real-time applications. Particularly, the good photostability of fluorescent material is significant for their application in the biological filed. The photostability of the synthesized CQDs was investigated by using the fluorometric method. As shown in Fig. 4(a), the final product of synthesized CQDs is yellowish in aqueous solution under the daylight and emitted intensive blue/cyan fluorescence under excitation of 365 nm UV light. The CQDs aqueous solution was exposed under the 365 nm UV light at the different irradiated time and then the fluorescence intensity of CQDs in aqueous solution was measured which is shown in Fig. 4(b). The fluorescence curve of CQDs does not exhibit obvious weakened fluorescence with UV exposure time 0–90 min. The intensity of the emission peak remained unchanged as that of the original intensity (0 min) even after being irritated for 90 min suggested that the synthesized CQDs showed excellent photostability for a longer time. This property makes the CQDs as good fluorescent probes for live-cell imaging, which may have a potential for microscopy and analytical applications [15].

In general, CQDs formation is suggested to proceed via four stages including dehydration, polymerization, carbonization, and passivation [39]. Herein, we proposed the preparation of CQDs from the banana peel with three stages including dehydration, polymerization, and carbonization as depicted in Scheme 2. Mostly, natural resources-derived CQDs were exhibited a strong fluorescence without any passivation. Although the formation of CQDs has been extensively investigated, the formation pathway is still unclear [40]. Banana peel possesses different phytoconstituents such as alkaloids, glycosides, saponins, tannins, flavonoids and so on which are essential in the formation of CQDs. Banana peel juice turned to fluorescent CQDs by the

hydrothermal process. In the first stage, phytoconstituents such as alkaloids, glycosides, saponins, tannins, and flavonoids undergo dehydration above 100 °C, presence of hydroxyl groups in phytoconstituents derived to formation of the furfural derivatives. The nitrogen-containing functionalities in phytoconstituents might react with carbonyl groups of phytoconstituents that will make stable complex. In the second stage, the dehydrated compounds will polymerized to form a linear and branched water-soluble polymers. In third stage, the water-soluble polymers and the stable complex of nitrogenized phytoconstituents will undergo carbonization which derived as functionalities of CQDs. The surface functionalities of CQDs are responsible for the solubility and good optical properties [41]. Optical performance and application of CQDs from waste banana peel compared with some other fluorescent CDs as shown in Table 1 [23,35,42–51]. It can be seen that the waste banana peel-derived CQDs showed better or comparable optical performance, including the multicolor fluorescence with quantum yield and bioimaging applications.

The fluorescent properties of CQDs were widely utilized for various biological applications. Compared to conventional organic dyes, CQDs are not suffering from photobleaching and photodegradation. Therefore, CQDs demonstrated great potential for cell imaging and labeling as a biocompatible fluorescent nanomaterial [52]. Due to excitation-dependent fluorescence emission, CQDs can be used as a multicolor nanoprobe that can be excited with different excitation wavelengths. The toxicity of CQDs is a natural concern for bioimaging applications [53]. Hence, the toxicity of CQDs was tested in live-cell lines (nematodes). MTT assay was used to perform the viability test at different CQDs concentrations from 0 to 200 μg mL^{-1}. Nematodes (Fig. 5 (a)) show a small decrease in viability (<5%). There is no significant loss in viability of nematodes even at higher concentrations of CQDs. This result is confirming that the synthesized CQDs exhibit good biocompatibility. Considering the above-mentioned properties such as intense fluorescence with excellent photostability, great water solubility and good biocompatibility of the synthesized CQDs, they are suitable candidates for bioimaging and other biomedical applications. The CQDs have been applied in *in-vivo* cellular studies using nematodes and corresponding microscopy images are shown as Fig. 5(b–f). The CQDs internalized into the nematodes and labeled not only the cell membrane and into the whole body of the nematodes. Besides, CQDs incubated nematodes have emitted blue, green, and red fluorescence upon 400, 470, and 550 nm excitation, respectively. The CQDs exhibit huge functional decoration on their surface which is inherent for the bonding of suitable nanomedicine. Subsequently, the nanomedicine bonded CQDs could be used for the targeted drug delivery because of their small size (~5 nm).

4. Conclusions

In summary, a novel CQDs have been synthesized through a simple hydrothermal carbonization method in an environment-friendly manner with the use of banana peel waste as both carbon and nitrogen sources. The resultant CQDs had near-spherical morphology with an average diameter of ~5 nm and exhibits an acceptable degree of graphitization. The biomass CQDs have excellent water solubility due to its functionality and showed bright fluorescence without further surface treatment with an acceptable quantum yield of 20%. Besides, CQDs have good biocompatibility and excellent fluorescence stability, which are ideal candidates for *in vivo* bioimaging applications. Their excitation-dependent fluorescence behaviors were successfully employed as an effective fluorescent probe in multicolor imaging applications of nematodes. More importantly, these results may motivate the cost-effective, green, and sustainable synthesis of highly fluorescent multifunctional carbon-based nanomaterials with various future potential applications such as biomedical and optoelectronic applications.

Author statement

Raji Atchudan: Conceptualization, Data curation, Funding acquisition, Investigation, Visualization, Writing - original draft. Thomas Nesakumar Jebakumar Immanuel Edison: Methodology, Resources and Validation. Mani Shanmugam: Formal analysis and Software. Suguna Perumal: Writing - review & editing. Thirunavukkarasu Somanathan: Formal analysis and Validation. Yong Rok Lee: Project administration and Supervision.

Declaration of competing interest

The authors declare that they have no known competing financial interests or personal relationships that could have appeared to influence the work reported in this paper.

Acknowledgments

This research was supported by the National Research Foundation (NRF) of Korea funded by the Ministry of Education, Science, and Technology (2012M3A7B4049675), the Ministry of Science, Information and Communications Technology (MSIT) (2017R1C1B5076345) and the MSIT (2018R1A2B2004432).

Appendix A. Supplementary data

Supplementary data to this article can be found online at https://doi.org/10.1016/j.physe.2020.114417.

References

[1] K. Raji, V. Ramanan, P. Ramamurthy, Facile and green synthesis of highly fluorescent nitrogen-doped carbon dots from jackfruit seeds and its applications towards the fluorimetric detection of Au3+ ions in aqueous medium and in in vitro multicolor cell imaging, New J. Chem. 43 (2019) 11710–11719.
[2] M. Pajewska-Szmyt, B. Buszewski, R. Gadzała-Kopciuch, Sulphur and nitrogen doped carbon dots synthesis by microwave assisted method as quantitative analytical nano-tool for mercury ion sensing, Mater. Chem. Phys. 242 (2020) 122484.
[3] C. Cheng, M. Xing, Q. Wu, A universal facile synthesis of nitrogen and sulfur co-doped carbon dots from cellulose-based biowaste for fluorescent detection of Fe3+ ions and intracellular bioimaging, Mater. Sci. Eng. C 99 (2019) 611–619.
[4] C. Cheng, M. Xing, Q. Wu, Preparation of carbon dots with long-wavelength and photoluminescence-tunable emission to achieve multicolor imaging in cells, Opt. Mater. 88 (2019) 353–358.
[5] C. Cheng, M. Xing, Q. Wu, Green synthesis of fluorescent carbon dots/hydrogel nanocomposite with stable Fe3+ sensing capability, J. Alloys Compd. 790 (2019) 221–227.
[6] A. Abbas, L.T. Mariana, A.N. Phan, Biomass-waste derived graphene quantum dots and their applications, Carbon 140 (2018) 77–99.
[7] F. Cui, Y. Ye, J. Ping, X. Sun, Carbon Dots: Current Advances in Pathogenic Bacteria Monitoring and Prospect Applications, Biosensors and Bioelectronics, 2020, p. 112085.
[8] R. Atchudan, T.N.J.I. Edison, K.R. Aseer, S. Perumal, N. Karthik, Y.R. Lee, Highly fluorescent nitrogen-doped carbon dots derived from Phyllanthus acidus utilized as a fluorescent probe for label-free selective detection of Fe3+ ions, live cell imaging and fluorescent ink, Biosens. Bioelectron. 99 (2018) 303–311.
[9] N.A. Mahat, S.A. Shamsudin, Transformation of oil palm biomass to optical carbon quantum dots by carbonisation-activation and low temperature hydrothermal processes, Diam. Relat. Mater. 102 (2020) 107660.
[10] J. Xu, L. Dai, C. Zhang, Y. Gui, L. Yuan, Y. Lei, B. Fan, Ionic liquid-aided hydrothermal treatment of lignocellulose for the synergistic outputs of carbon dots and enhanced enzymatic hydrolysis, Bioresour. Technol. 305 (2020) 123043.
[11] S. Chernyak, A. Podgornova, S. Dorofeev, S. Maksimov, K. Maslakov, S. Savilov, V. Lunin, Synthesis and modification of pristine and nitrogen-doped carbon dots by combining template pyrolysis and oxidation, Appl. Surf. Sci. 507 (2020) 145027.
[12] G. Liu, B. Li, Y. Liu, Y. Feng, D. Jia, Y. Zhou, Rapid and high yield synthesis of carbon dots with chelating ability derived from acrylamide/chitosan for selective detection of ferrous ions, Appl. Surf. Sci. 487 (2019) 1167–1175.
[13] J. Li, K. Tang, J. Yu, H. Wang, M. Tu, X. Wang, Nitrogen and chlorine co-doped carbon dots as probe for sensing and imaging in biological samples 6, Royal Society Open Science, 2019, p. 181557.
[14] B. Xue, Y. Yang, Y. Sun, J. Fan, X. Li, Z. Zhang, Photoluminescent lignin hybridized carbon quantum dots composites for bioimaging applications, Int. J. Biol. Macromol. 122 (2019) 954–961.

[15] R. Atchudan, T.N.J.I. Edison, S. Perumal, N. Muthuchamy, Y.R. Lee, Eco-friendly synthesis of tunable fluorescent carbon nanodots from Malus floribunda for sensors and multicolor bioimaging, J. Photochem. Photobiol. Chem. 390 (2020) 112336.
[16] V.N. Mehta, S. Jha, H. Basu, R.K. Singhal, S.K. Kailasa, One-step hydrothermal approach to fabricate carbon dots from apple juice for imaging of mycobacterium and fungal cells, Sensor. Actuator. B Chem. 213 (2015) 434–443.
[17] R. Atchudan, T.N.J.I. Edison, S. Perumal, R. Vinodh, Y.R. Lee, Betel-derived nitrogen-doped multicolor carbon dots for environmental and biological applications, J. Mol. Liq. 296 (2019) 111817.
[18] Q. Huang, Q. Li, Y. Chen, L. Tong, X. Lin, J. Zhu, Q. Tong, High quantum yield nitrogen-doped carbon dots: green synthesis and application as "off-on" fluorescent sensors for the determination of Fe3+ and adenosine triphosphate in biological samples, Sensor. Actuator. B Chem. 276 (2018) 82–88.
[19] F. Huo, Z. Kang, M. Zhu, C. Tan, Y. Tang, Y. Liu, W. Zhang, Metal-triggered fluorescence enhancement of multicolor carbon dots in sensing and bioimaging, Opt. Mater. 94 (2019) 363–370.
[20] J. Ahn, Y. Song, J.E. Kwon, S.H. Lee, K.S. Park, S. Kim, J. Woo, H. Kim, Food waste-driven N-doped carbon dots: applications for Fe3+ sensing and cell imaging, Mater. Sci. Eng. C 102 (2019) 106–112.
[21] A. Mary Alex, M.D. Kiran, G. Hari, A. Krishnan, J.S. Jayan, A. Saritha, Carbon dots: a green synthesis from Lawsonia inermis leaves, Mater. Today: Proceedings 26 (2020) 716–719.
[22] R. Atchudan, T.N.J.I. Edison, M.G. Sethuraman, Y.R. Lee, Efficient synthesis of highly fluorescent nitrogen-doped carbon dots for cell imaging using unripe fruit extract of Prunus mume, Appl. Surf. Sci. 384 (2016) 432–441.
[23] R. Atchudan, T.N. Jebakumar Immanuel Edison, S. Perumal, R. Vinodh, Y.R. Lee, Multicolor-emitting carbon dots from Malus floribunda and their interaction with Caenorhabditis elegans, Mater. Lett. 261 (2020) 127153.
[24] L. Chen, C. Iwamoto, E. Omurzak, S. Takebe, H. Okudera, A. Yoshiasa, S. Sulaimankulova, T. Mashimo, Synthesis of zirconium carbide (ZrC) nanoparticles covered with graphitic "windows" by pulsed plasma in liquid, RSC Adv. 1 (2011) 1083–1088.
[25] R. Atchudan, T.N.J.I. Edison, D. Chakradhar, S. Perumal, J.-J. Shim, Y.R. Lee, Facile green synthesis of nitrogen-doped carbon dots using Chionanthus retusus fruit extract and investigation of their suitability for metal ion sensing and biological applications, Sensor. Actuator. B Chem. 246 (2017) 497–509.
[26] H. Eskalen, S. Uruş, S. Cömertpay, A.H. Kurt, Ş. Özgan, Microwave-assisted ultra-fast synthesis of carbon quantum dots from linter: fluorescence cancer imaging and human cell growth inhibition properties, Ind. Crop. Prod. 147 (2020) 112209.
[27] J. Zhong, X. Chen, M. Zhang, C. Xiao, L. Cai, W.A. Khan, K. Yu, J. Cui, L. He, Blood compatible heteratom-doped carbon dots for bio-imaging of human umbilical vein endothelial cells, Chin. Chem. Lett. 31 (2020) 769–773.
[28] R. Atchudan, T.N.J.I. Edison, S. Perumal, N. Clament Sagaya Selvam, Y.R. Lee, Green synthesized multiple fluorescent nitrogen-doped carbon quantum dots as an efficient label-free optical nanoprobe for in vivo live-cell imaging, J. Photochem. Photobiol. Chem. 372 (2019) 99–107.
[29] D.Y. Li, S.P. Wang, F. Azad, S.C. Su, Single-step synthesis of polychromatic carbon quantum dots for macroscopic detection of Hg2+, Ecotoxicol. Environ. Saf. 190 (2020) 110141.
[30] R. Atchudan, T.N.J.I. Edison, K.R. Aseer, S. Perumal, Y.R. Lee, Hydrothermal conversion of Magnolia liliiflora into nitrogen-doped carbon dots as an effective turn-off fluorescence sensing, multi-colour cell imaging and fluorescent ink, Colloids Surf. B Biointerfaces 169 (2018) 321–328.
[31] X.-D. Mai, T. Thi Kim Chi, T.-C. Nguyen, V.-T. Ta, Scalable synthesis of highly photoluminescence carbon quantum dots, Mater. Lett. 268 (2020) 127595.
[32] J. Ju, W. Chen, Synthesis of highly fluorescent nitrogen-doped graphene quantum dots for sensitive, label-free detection of Fe (III) in aqueous media, Biosens. Bioelectron. 58 (2014) 219–225.
[33] R. Atchudan, N. Muthuchamy, T.N.J.I. Edison, S. Perumal, R. Vinodh, K.H. Park, Y. R. Lee, An ultrasensitive photoelectrochemical biosensor for glucose based on bio-derived nitrogen-doped carbon sheets wrapped titanium dioxide nanoparticles, Biosens. Bioelectron. 126 (2019) 160–169.
[34] Z.-F. Pu, Q.-L. Wen, Y.-J. Yang, X.-M. Cui, J. Ling, P. Liu, Q.-E. Cao, Fluorescent carbon quantum dots synthesized using phenylalanine and citric acid for selective detection of Fe3+ ions, Spectrochim. Acta Mol. Biomol. Spectrosc. 229 (2020) 117944.
[35] R. Atchudan, T.N.J.I. Edison, Y.R. Lee, Nitrogen-doped carbon dots originating from unripe peach for fluorescent bioimaging and electrocatalytic oxygen reduction reaction, J. Colloid Interface Sci. 482 (2016) 8–18.
[36] P. Brachi, Synthesis of carbon dots (CDs) through the fluidized bed thermal treatment of residual biomass assisted by γ-alumina, Appl. Catal. B Environ. 263 (2020) 118361.
[37] R. Zhang, W. Chen, Nitrogen-doped carbon quantum dots: facile synthesis and application as a "turn-off" fluorescent probe for detection of Hg2+ ions, Biosens. Bioelectron. 55 (2014) 83–90.
[38] R. Atchudan, T.N.J.I. Edison, S. Perumal, M. Shanmugam, Y.R. Lee, Facile one-pot synthesis of novel structured IONP@C-HIOP composite as superior electrocatalyst for hydrogen evolution reaction and aqueous waste investigation of bio-imaging applications, J. Mol. Liq. 268 (2018) 343–353.
[39] P.-C. Hsu, H.-T. Chang, Synthesis of high-quality carbon nanodots from hydrophilic compounds: role of functional groups, Chem. Commun. 48 (2012) 3984–3986.
[40] S. Sahu, B. Behera, T.K. Maiti, S. Mohapatra, Simple one-step synthesis of highly luminescent carbon dots from orange juice: application as excellent bio-imaging agents, Chem. Commun. 48 (2012) 8835–8837.
[41] T.N.J.I. Edison, R. Atchudan, J.-J. Shim, S. Kalimuthu, B.-C. Ahn, Y.R. Lee, Turn-off fluorescence sensor for the detection of ferric ion in water using green synthesized N-doped carbon dots and its bio-imaging, J. Photochem. Photobiol. B Biol. 158 (2016) 235–242.
[42] C. Wang, H. Shi, M. Yang, Y. Yan, E. Liu, Z. Ji, J. Fan, Facile synthesis of novel carbon quantum dots from biomass waste for highly sensitive detection of iron ions, Mater. Res. Bull. 124 (2020) 110730.
[43] L. Li, R. Zhang, C. Lu, J. Sun, L. Wang, B. Qu, T. Li, Y. Liu, S. Li, In situ synthesis of NIR-light emitting carbon dots derived from spinach for bio-imaging applications, J. Mater. Chem. B 5 (2017) 7328–7334.
[44] H. Diao, T. Li, R. Zhang, Y. Kang, W. Liu, Y. Cui, S. Wei, N. Wang, L. Li, H. Wang, W. Niu, T. Sun, Facile and green synthesis of fluorescent carbon dots with tunable emission for sensors and cells imaging, Spectrochim. Acta Mol. Biomol. Spectrosc. 200 (2018) 226–234.
[45] P. Das, S. Ganguly, P.P. Maity, M. Bose, S. Mondal, S. Dhara, A.K. Das, S. Banerjee, N.C. Das, Waste chimney oil to nanolights: a low cost chemosensor for tracer metal detection in practical field and its polymer composite for multidimensional activity, J. Photochem. Photobiol. B Biol. 180 (2018) 56–67.
[46] J.R. Bhamore, S. Jha, T.J. Park, S.K. Kailasa, Green synthesis of multi-color emissive carbon dots from Manilkara zapota fruits for bioimaging of bacterial and fungal cells, J. Photochem. Photobiol. B Biol. 191 (2019) 150–155.
[47] S.K. Kailasa, S. Ha, S.H. Baek, L.M.T. Phan, S. Kim, K. Kwak, T.J. Park, Tuning of carbon dots emission color for sensing of Fe3+ ion and bioimaging applications, Mater. Sci. Eng. C 98 (2019) 834–842.
[48] Y. Liu, C. Zhu, Y. Gao, L. Yang, J. Xu, X. Zhang, C. Lu, Y. Wang, Y. Zhu, Biomass-derived nitrogen self-doped carbon dots via a simple one-pot method: physicochemical, structural, and luminescence properties, Appl. Surf. Sci. 510 (2020) 145437.
[49] C. Zhang, Y. Xiao, Y. Ma, B. Li, Z. Liu, C. Lu, X. Liu, Y. Wei, Z. Zhu, Y. Zhang, Algae biomass as a precursor for synthesis of nitrogen-and sulfur-co-doped carbon dots: a better probe in Arabidopsis guard cells and root tissues, J. Photochem. Photobiol. B Biol. 174 (2017) 315–322.
[50] Z. Liu, W. Jin, F. Wang, T. Li, J. Nie, W. Xiao, Q. Zhang, Y. Zhang, Ratiometric fluorescent sensing of Pb2+ and Hg2+ with two types of carbon dot nanohybrids synthesized from the same biomass, Sensor. Actuator. B Chem. 296 (2019) 126698.
[51] H. Qi, M. Teng, M. Liu, S. Liu, J. Li, H. Yu, C. Teng, Z. Huang, H. Liu, Q. Shao, A. Umar, T. Ding, Q. Gao, Z. Guo, Biomass-derived nitrogen-doped carbon quantum dots: highly selective fluorescent probe for detecting Fe3+ ions and tetracyclines, J. Colloid Interface Sci. 539 (2019) 332–341.
[52] T.S. Atabaev, Doped carbon dots for sensing and bioimaging applications, A Minireview, Nanomaterials (Basel) 8 (2018) 342.
[53] J. Ju, R. Zhang, S. He, W. Chen, Nitrogen-doped graphene quantum dots-based fluorescent probe for the sensitive turn-on detection of glutathione and its cellular imaging, RSC Adv. 4 (2014) 52583–52589.